# GPU Acceleration of the Material Point Method

Fabian Meyer

University of Koblenz

Kolloquium Computergrafik, 14 February 2019

# A Brief MPM Overview: Do You Want to Build a Snowman?

A short historical summary of MPM:

- Belongs to family of particle-in-cell(PIC) techniques [EHB57].
- Initial application to solids [SZS95] → MPM
- From research to production in *Disney's* animation film *Frozen* [Sto+13].
- Avalanche research [Gau+18]

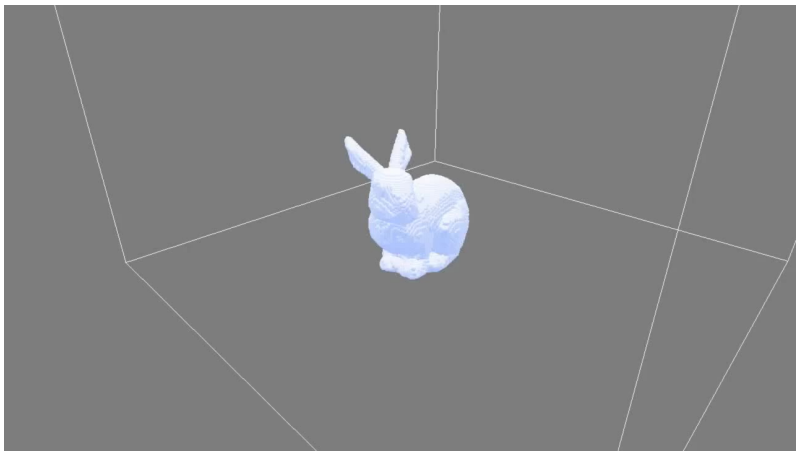

Video result of my bachelor thesis on the simulation of snow [Mey15].

PIC ideas:

- Combine Lagrangian particles & Eulerian grid
- Particles store all information

Typical PIC/MPM roundtrip:

1. Particle-to-grid(P2G) transfer to an unmoving grid
2. Solve discretized governing equations on grid
3. Grid-to-particle(G2P) transfer back to particles & move them

$\Rightarrow$ **meshfree, non-empirical**

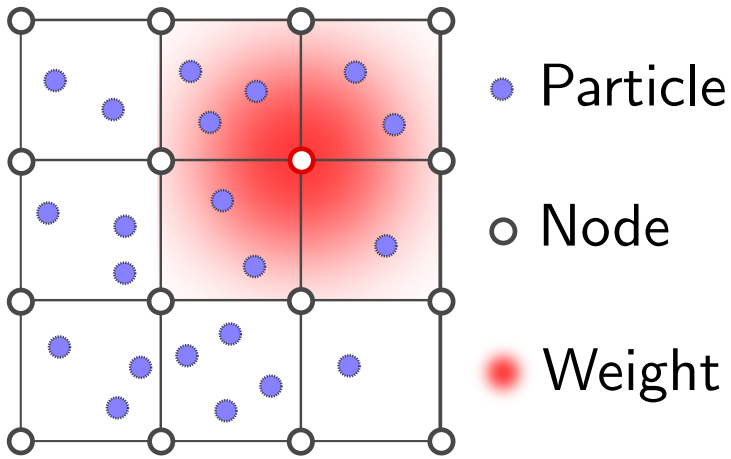


Transfers: Interpolation functions are defined over grid nodes.

## GPGPU for performance enthusiasts

Why would('nt) you?

**Drawbacks:**

- Interactivity much easier on CPU, but slow PCI-Bus communication
- Code is mostly written against GPU architecture
- A lot of strain on the programmer

**Benefits:**

- Data is already on the GPU for rendering
- **Higher parallelization acceleration**

# Governing Equations: Conservation of Mass & Momentum

**Conservation of mass**, continuum assumption holds.
Lagrangian (moving with a particle ${}_0\boldsymbol{x}$):

$$ {}^t_0 J \rho({}_0\boldsymbol{x}, t) = \rho({}_0\boldsymbol{x}, 0). \tag{1} $$

Eulerian (outside observer ${}_t\boldsymbol{x}$):

$$ \frac{\partial}{\partial t} \rho({}_t\boldsymbol{x}, t) = -\vec{\nabla} \cdot (\rho({}_t\boldsymbol{x}, t) \boldsymbol{v}({}_t\boldsymbol{x}, t)). \tag{2} $$

Lagrangian and Eulerian view measure differently but give same results. Equations are given in the strong form! [Jia+16][Abe12]

**Conservation of momentum**:
Lagrangian (moving with a particle ${}_0\boldsymbol{x}$):

$$\rho({}_0\boldsymbol{x}, 0)\boldsymbol{a}({}_0\boldsymbol{x}, t) = \vec{\nabla} \cdot \boldsymbol{P}({}_0\boldsymbol{x}, t) + \boldsymbol{f}^{\text{body}}({}_0\boldsymbol{x}, t){}_0^t J. \tag{3}$$

Eulerian (outside observer ${}_t\boldsymbol{x}$):

$$\rho({}_t\boldsymbol{x}, t)\boldsymbol{a}({}_t\boldsymbol{x}, t) = \vec{\nabla} \cdot \boldsymbol{\sigma}({}_t\boldsymbol{x}, t) + \boldsymbol{f}^{\text{body}}({}_t\boldsymbol{x}, t) \tag{4}$$

Solving this equation will tell us how the velocity fields $\boldsymbol{v}({}_t\boldsymbol{x}), \boldsymbol{v}({}_0\boldsymbol{x})$ change on the whole domain due to acceleration $\boldsymbol{a}$.
This is important to advect particles accounting for all forces.
[Jia+16][Abe12]

## The Pretty Strong but Mathematically Weak Formulation

**Weak Formulation** (or Principle of Virtual Work):
Dot product equations with arbitrarily 'test functions' $\boldsymbol{q}$ and apply divergence theorem:

$$\int_{\Omega^0} {}_0\boldsymbol{q} \cdot \left[ ({}_0\rho_0)({}_0\boldsymbol{a}) - {}_0\boldsymbol{f}^{\text{body}} {}^t_0 J \right] d_0\boldsymbol{x} = \int_{\partial\Omega^{t^n}} {}_t\boldsymbol{q} \cdot \boldsymbol{\sigma} d_t\boldsymbol{A} - \int_{\Omega^{t^n}} \nabla_t \boldsymbol{q} : \boldsymbol{\sigma} d_t\boldsymbol{x}. \quad (5)$$

A strong solution is also a solution to the weak formulation. Leave out body forces(like gravity) and boundary condition (e.g. collisions) for now:

$$\int_{\Omega^0} {}_0\boldsymbol{q} \cdot ({}_0\rho_0)({}_0\boldsymbol{a}) d_0\boldsymbol{x} = \int_{\Omega^{t^n}} \nabla_t \boldsymbol{q} : \boldsymbol{\sigma} d_t\boldsymbol{x}. \quad (6)$$

## **Weak Derivative**:

$y = |t|$ has weak derivative:

$$v = \begin{cases} -1, & \text{if } t < 0 \\ c, & \text{if } t = 0 \\ 1, & \text{if } t > 0 \end{cases}$$

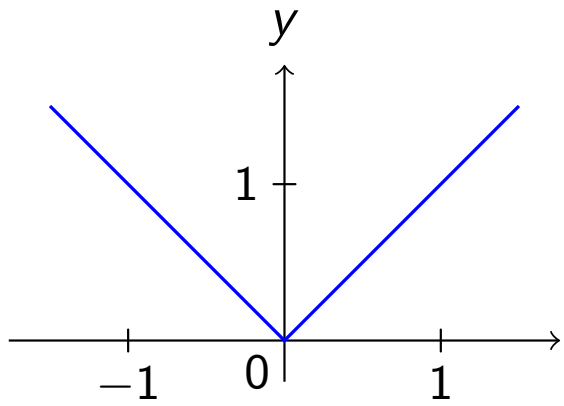


Heaviside step function has no weak derivate:

$$s = \begin{cases} 0, & \text{if } t < 0 \\ 1, & \text{if } t \geq 0 \end{cases}$$

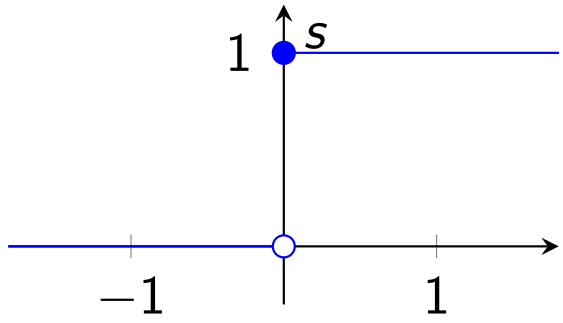


Allows for point loads, material discontinuities and more. [Bat06]

## Discretization of Space and Time

**Time discretization** with implicit midpoint scheme:

$$\frac{y^{n+1} - y^n}{\Delta t} = f^{n+\frac{1}{2}} = f\left(t^n + \frac{\Delta t}{2}, \frac{1}{2}y^n + \frac{1}{2}y^{n+1}\right) \tag{7}$$

- **implicit** requires linear system solve $\Rightarrow$ more stable, larger time steps
- **midpoint** as it conserves gov. equations

$$\Rightarrow \int_{\Omega^t} {}_t\boldsymbol{q} \cdot {}_t\rho({}_t\boldsymbol{v}^{n+1} - {}_t\boldsymbol{v}^n) d_t\boldsymbol{x} = \int_{\Omega^{t^n}} \nabla {}_t\boldsymbol{q} : \boldsymbol{\sigma}^{n+\frac{1}{2}} d_t\boldsymbol{x}. \tag{8}$$

**Space Discretization** is done in a Galerkin/FEM fashion with grid based interpolants $w_i$ with limited support. Here dyadic products

$$w_i(\boldsymbol{x}) = w(\boldsymbol{x} - \boldsymbol{x}_i) = w(\frac{1}{h}(x - x_i))w(\frac{1}{h}(y - y_i)w(\frac{1}{h}(z - z_i)) \quad (9)$$

of cubic b-splines suffice:

$$w(x) = \begin{cases} \frac{1}{2}|x|^3 - |x|^2 + \frac{2}{3} & 0 \leqslant |x| < 1 \\ \frac{1}{6}(2 - |x|)^3 & 1 \leqslant |x| < 2 \\ 0 & 2 \leqslant |x| \end{cases} . \quad (10)$$

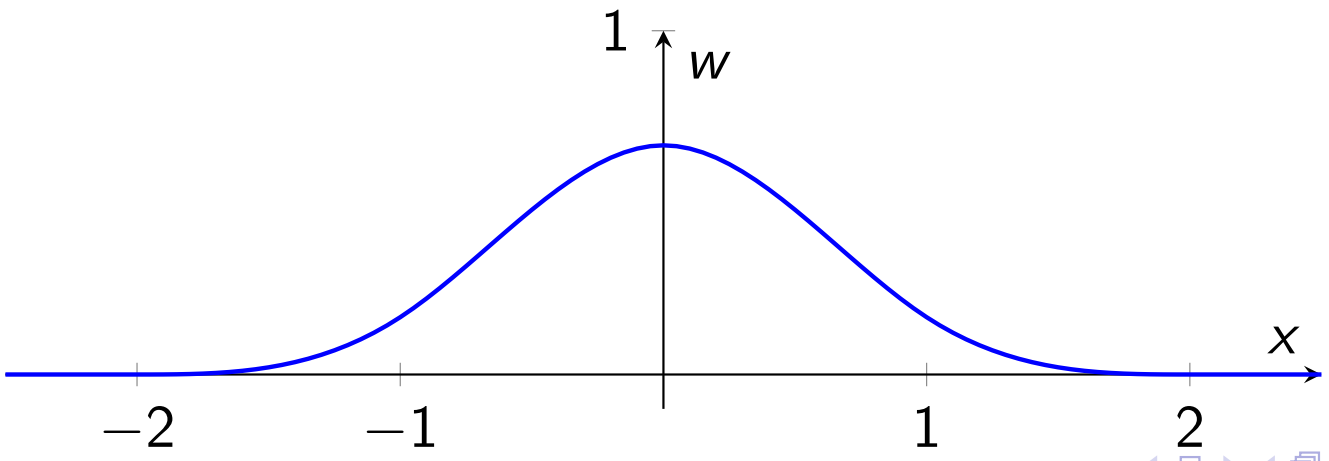

Thus set in:

$$ {}_t\boldsymbol{q}(\boldsymbol{x}, t^n) = \sum_i \boldsymbol{e}_i w_i(\boldsymbol{x}), {}_t\boldsymbol{v}^{n(+1)}(\boldsymbol{x}) = \sum_j \boldsymbol{v}_j^{n(+1)} w_j(\boldsymbol{x}). $$

Combine it with numerical integration where the particles function as quadrature points [SKB08]:

$$ \begin{aligned} g_i &= \int_\Omega g(\boldsymbol{x}) w_i(\boldsymbol{x}) d\boldsymbol{x} \\ &\approx \sum_p g_p w_i(\boldsymbol{x}_p) V_p. \end{aligned} \tag{11} $$

due to integration by midpoint rule:

$$ \int_\Omega f(x) dx \approx \sum_{i=1}^{N} f(x_i) h_i. \tag{12} $$

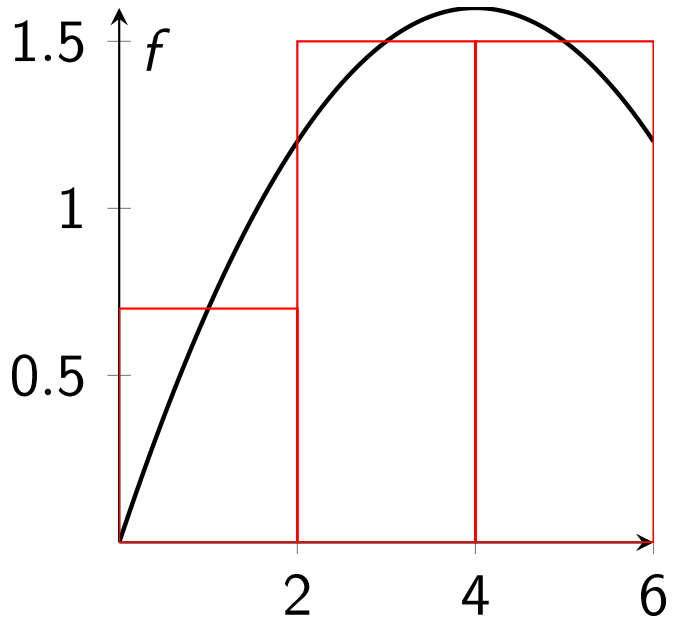

# Velocity Fields: APIC-Transfers

PIC-transfer

1. $(m\boldsymbol{v})_i^n = \sum_p w_{ip}^n m_p \boldsymbol{v}_p^n$
2. $\boldsymbol{v}_i^n = \frac{(m\boldsymbol{v})_i^n}{m_i^n}$
3. $\boldsymbol{v}_{p,PIC}^{n+1} = \sum_i w_{ip}^n \boldsymbol{v}_i^{n+1}$

APIC-transfers add a local velocity field $\boldsymbol{C}_p^n$ around $\boldsymbol{v}_p^n$:

$(m\boldsymbol{v})_i^n = \sum_p w_{ip}^n m_p \left(\boldsymbol{v}_p^n + \boldsymbol{C}_p^n(\boldsymbol{x}_i^n - \boldsymbol{x}_p^n)\right)$

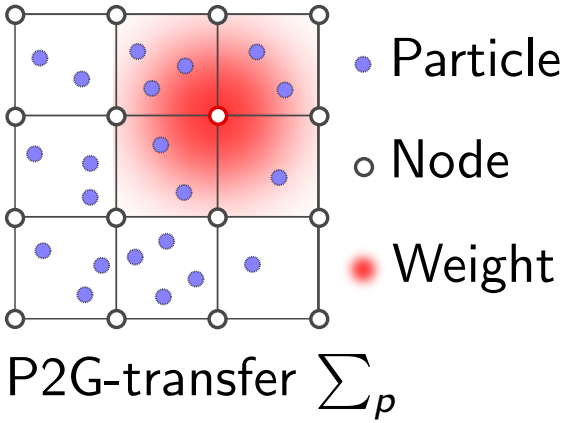


P2G-transfer $\sum_p$

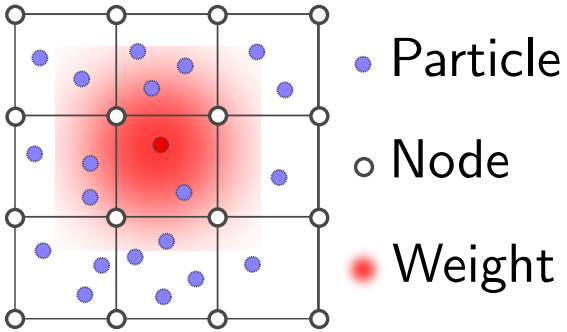


G2P-transfer $\sum_i$

# Layout of the data: SoA vs. AoS

## Coalescing:

SoA-Layout

```
struct Container{
  vec4 positions[n];
  vec4 velocities[n];
} Particles;
```

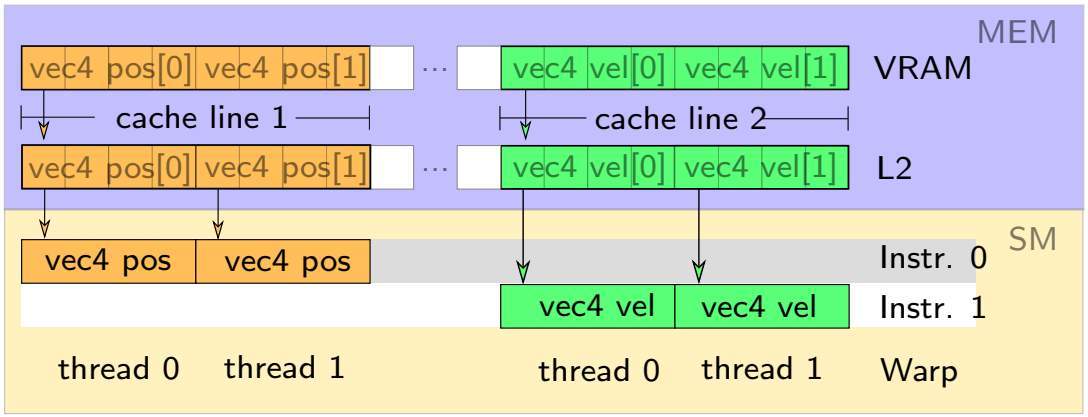


Structures of arrays(SoA)

AoS-Layout

```
struct Particle {
  vec4 position;
  vec4 velocity;
} Particles[n];
```

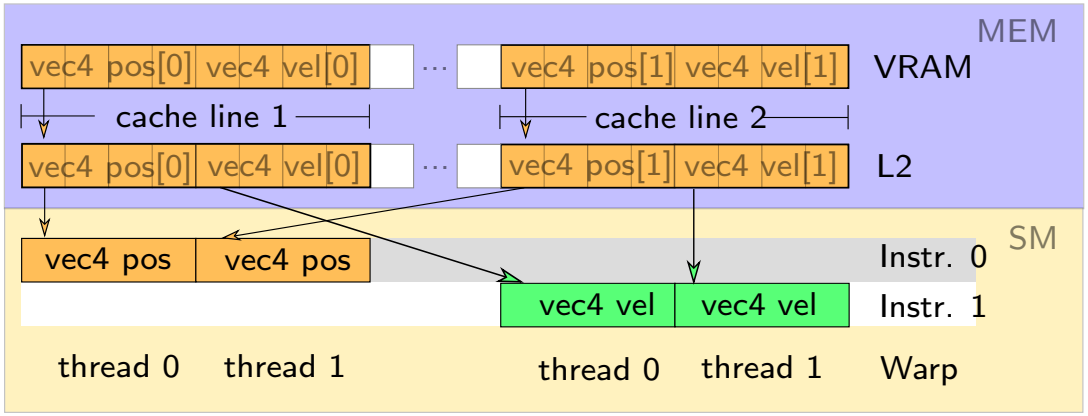


Arrays of structures(AoS)

Nvidia Nsight[NVI] now offers metrics to identify bottlenecks:

| **Metric** | **Description** |
|---|---|
| VRAM SOL% | memory througput w.r.t. to hardware limit |
| SM SOL% | instruction throughput |
| L2 SOL% | L2-cache throughput |
| Tex SOL% | L1-cache throughput |
| SM Issue Util.% | amount of cycles an instr. was issued |

A simple map(`y=length(x)`) shader on 1024×1024 Elements SoA vs. AoS differences:

| Layout | $\Delta t_c(\mu s)$ | Speedup | VRAM | SM | L2 | SM Issue Util. |
|---|---|---|---|---|---|---|
| AoS(1 instr.) | 243 | - | 77.7% | 7.3% | 30.3% | 6.8% |
| SoA(1 instr.) | **120** | 2.26x | 75.4% | **14.3%** | 29.4% | **14.0%** |
| AoS(2 instr.) | 275 | - | 61.3% | **41.8%** | **53.8%** | 48.9% |
| SoA(2 instr.) | 240 | 1.16x | 75.4% | 29.4% | 20.0% | 62.3% |

⇒ SoA increases coalescing for non-random access.

## Parallel Reduction & Scan

Assuming an associative `binary_op(x,y)`$:= x \circ y$ , a neutral element $e$ of the `binary_op`, and an array of values $[a_0, a_1, ..., a_n]$.

- **Parallel reduction** computes the value:

$$r = a_0 \circ a_1 \circ ... \circ a_n. \tag{13}$$

- (Exclusive) **scan** computes the array:

$$[e, a_0, (a_0 \circ a_1), (a_0 \circ a_1 \circ a_2), \ ... \ , (a_0 \circ a_1 \circ a_2 \circ ... \circ a_{n-1})]. \tag{14}$$

Here, only shared memory approaches without (NVIDIA exclusive) warp shuffle operations.

# Shared Memory Bank Conflicts:

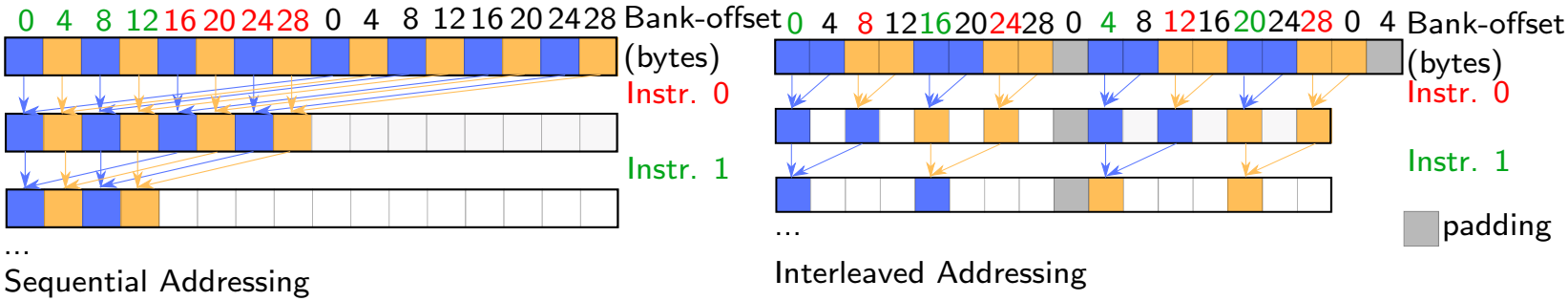


Interleaved addressing causes bank conflicts (Short Scoreboard activity) $\Rightarrow$ padding needed.

| Method | $\Delta t_c$ | Speedup | VRAM | SM | Sel. Warp-Stall Reas. |
|---|---|---|---|---|---|
| Interl. no padd. | 305 | - | 23.0% | **60.9%** | S. Scoreb.(17.2%) |
| Sequential | 141 | 2.16x | **49.8%** | 37.1% | **S. Scoreb.(2.0%)** |

Table: Parallel reduction on $1024 \times 1024$ vectors with `y=length(x)` as input.

More elements than thread group size require pyramid schemes.

**Sequential work**: multiple elements per thread.

- Memory latency hiding (Long Scoreboard up)
- Higher reduction factor each dispatch ⇒ Less global memory indirections
- Unrolling loops can help but adds register pressure.

| Method | $\Delta t_c$ | Speedup | VRAM | SM | Sel. Warp-Stall Reas. |
|---|---|---|---|---|---|
| Sequential | 141 | 2.16x | 49.8% | 37.1% | S. Scoreb.(2.0%) |
| Seq. (2x) | 100 | 3.05x | 69.5% | 26.2% | L. Scoreb.(80.1%) |
| Seq. (128x) | 98 | 3.1x | **72.9%** | 16.9% | **L. Scoreb.(84.4%)** |
| Seq. (256x) | 101 | 3.0x | 66.4% | 14.6% | L. Scoreb.(76.9%) |

Table: Parallel reduction on $1024 \times 1024$ vectors with `y=length(x)` as input. Methods have 504, 8, 4 thread groups, respectively. A GTX970 has 13 SMs.

Scan is similar but cannot profit as much from sequential work having to keep multiple elements in register memory.

# Binning & Counting Sort: Where Are You?

Grid node does not know its neighboring particles ⇒ Binning.

Binning combines nicely with **Counting Sort:**

1. **Binning**: Per node counting.
2. **Scan**: Computes new memory offset for particles.
3. **Reordering**: Give back indexing list or do deep copy.

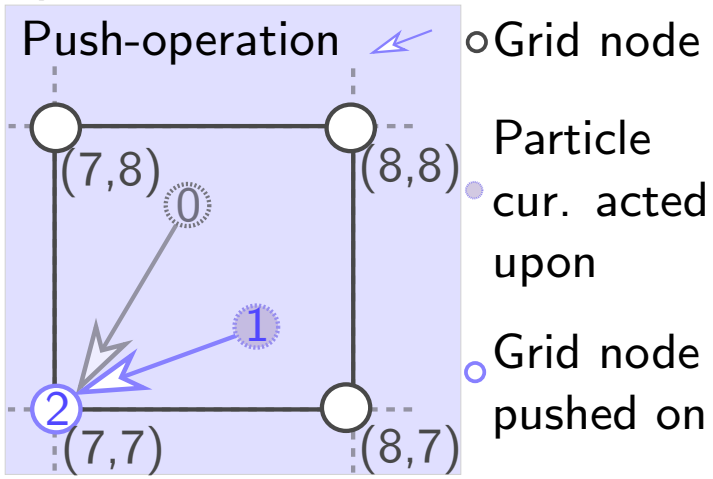

Sorting can dramatically increase workload performance of subsequent steps for neighboring queries:

1. Deep sorted accesses are now **coalesced**.
2. **Data reuse** due to L2-Cache and/or shared memory.

**Double buffer particles** to use last sorted state as input for new sorting to profit from item 1 and 2!

| Ordering | $\Delta t_c(\mu s)$ | Speedup | VRAM | SM | L2 | L2-Hit |
|---|---|---|---|---|---|---|
| Random | 1,516 | - | 25.0% | 3.4% | 9.1% | 10.8% |
| Deep sorted | 218 | 6.95x | **75.3%** | 24.4% | **35.0%** | **37.8%** |

Table: Order dependency of binning of $1024 \times 1024$ randomly positioned particles in a $128 \times 128 \times 128$ grid.

## The MPM Specific Transfers

All MPM operations belong to one of those parallelization schemes:

- 1 thread : 1 particle: $\square_p = \square_p \circ \square_p \circ ... \circ \square_p$.
- 1 thread : 1 node: $\square_p = \square_p \circ \square_p \circ ... \circ \square_p$.
- G2P-transfer: $\square_p = \sum_i \square_i \circ \square_{ip}$.
- P2G-transfer: $\square_i = \sum_p \square_p \circ \square_{ip}$.

MPM-Transfers are executed **multiple times per physical frame** with varying numbers of variables and mathematical operations.

$\Rightarrow$ Preprocessing steps only need to be done **once per physical frame**. Sorting already introduced as one of these.

G2P-Transfer: $\square_p = \sum_i \square_i \circ \square_{ip}$.

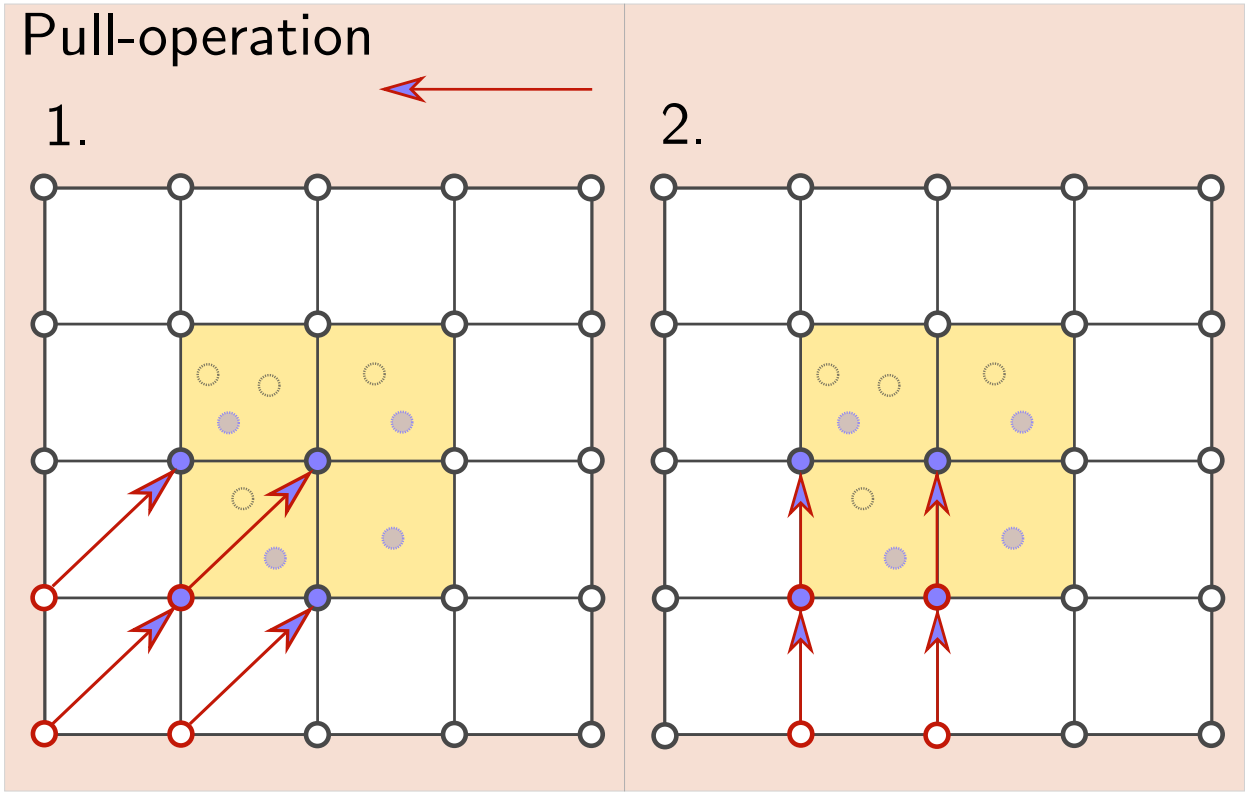


Pull-Operations read!

Similar to filter or stencil operations on the GPU:

- 1 node : 1 thread, split grid into blocks corr. to thread groups.
- Interpolation function however dependent on particle position.
- Needs to be rerun for every particle in the cell.

Typical setup of transfers:

1. Initialize shared memory (pull: with nodes from global memory).
2. Perform transfers.
3. Write back to global memory (push: global atomics since writes on halo).

P2G-transfer: $\square_i = \sum_p \square_p \circ \square_{ip}$.

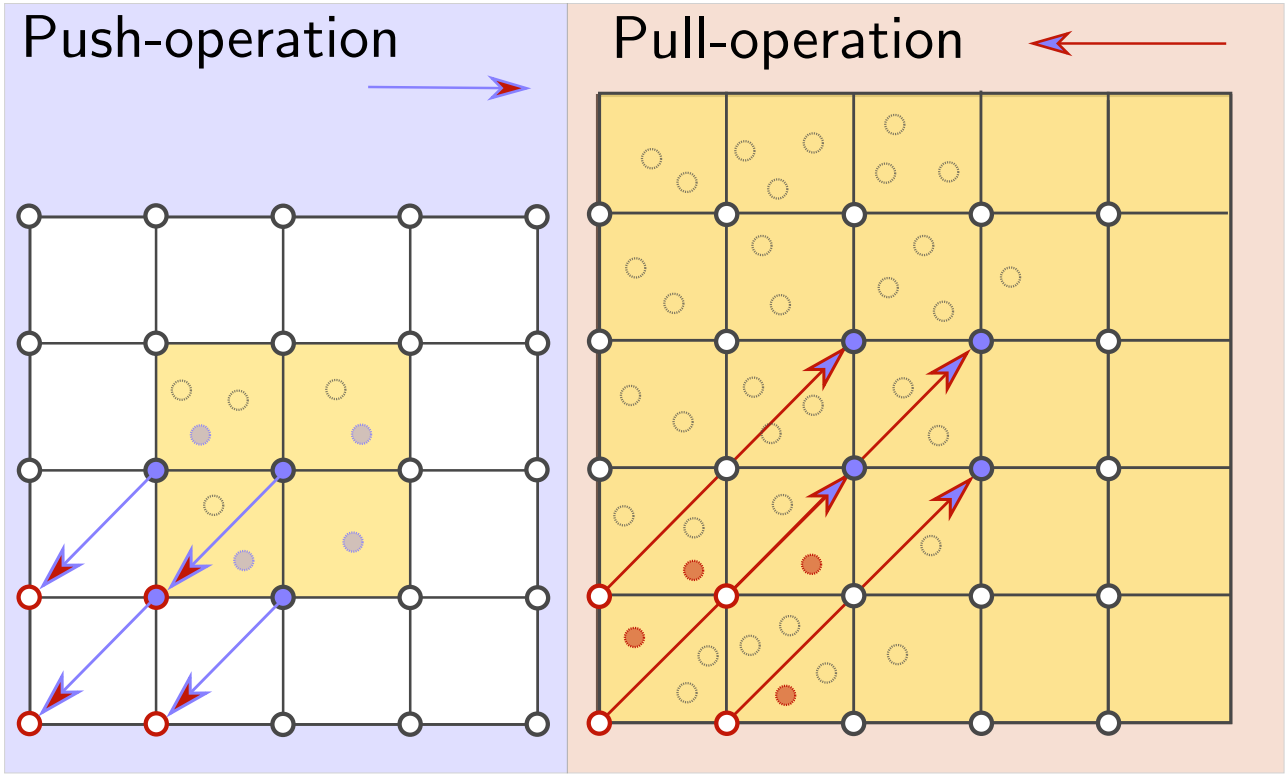


Pull-Operations read, Push-operations write!

$\Rightarrow$ Race conditions.

Typically simulation domain(grid) much bigger than simulation model. Filtering inactive blocks as a preprocess improves performance.

- Block is active if any cell counter is active.
- Cell counter is active if it has at least one particle.

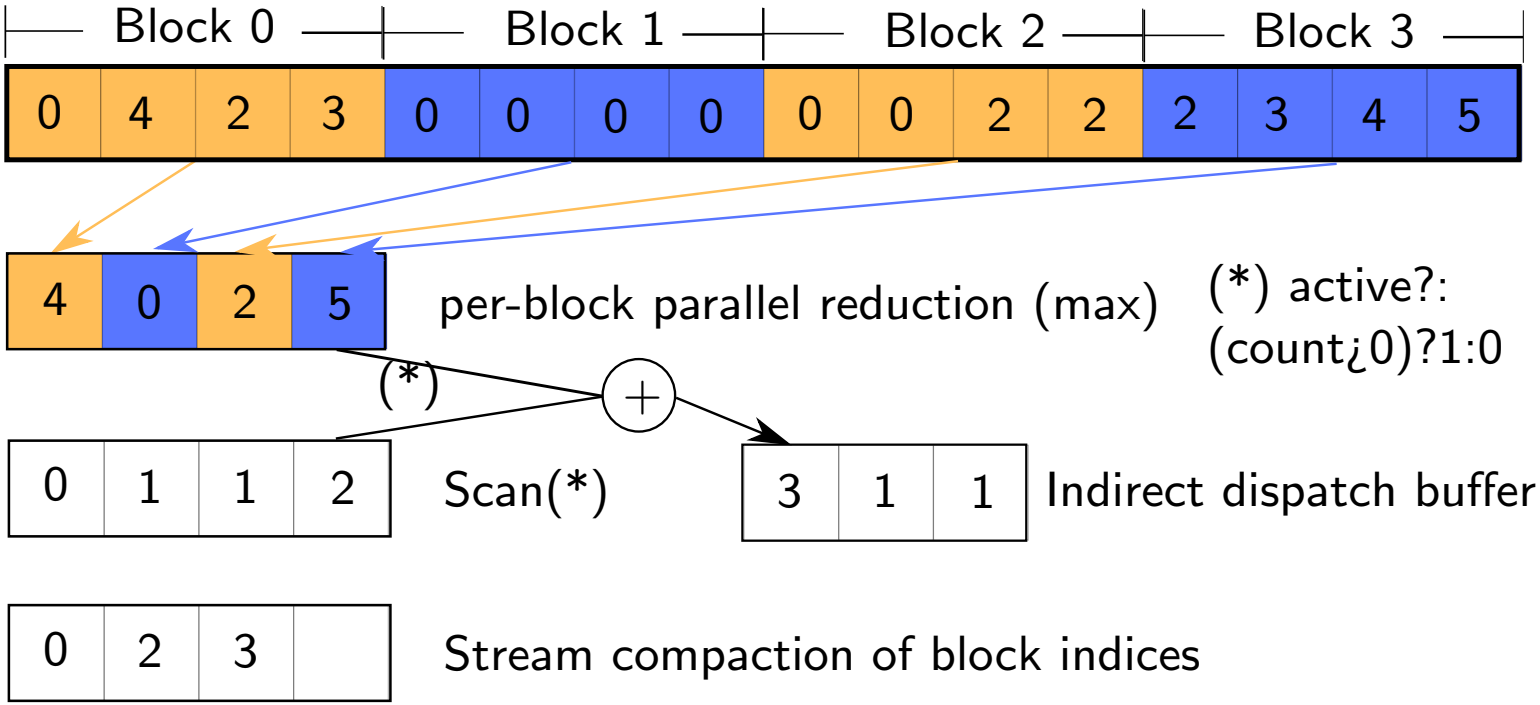

- Block and its halo are always target of shared memory operations $\Rightarrow$ P2G-Pull low occupancy.
- Batching multiple particles can increase performance due to hiding synchronization, unroll!
- Transfers respect shared memory bank conflicts fully.
- Warp divergence for varying cell counts.

| Method | $\Delta t_c(\mu s)$ | Speedup | VRAM | L2 | SM |
|---|---|---|---|---|---|
| global | 44,442 | - | 4.6 % | 34.4% | 7.7% |
| global sorted | 20,484 | 2.21x | 7.0 % | **44.0%** | 16.1% |
| P2G-sync | **2,595** | 17.47x | 5.9% | 7.6% | **67.0%** |

P2G-transfers of one uniformly million particles with 4 particles per cell with random velocities between $v_x, v_y, v_z \in [-1.0; 1.0]$ in a $128 \times 128 \times 128$ grid. Block size is (8,4,4).

# A comparison to [Gao+18]

Largely same decision making:

| | Me | [Gao+18] |
|---|---|---|
| Sort | Count/Histogram for each var. | Count/Histogram sel. variables |
| Filtering domain | Filter-op. | Sparse Grid structure |
| Transfers | Shared mem. only | Warp-shuffle op. |

Warp shuffle allows for fast parallel segmented reduction of cells of varying counts.
$\Rightarrow$ Solves warp divergence and shared memory issues mostly, thread groups now correspond to particles. Faster in these instances but NVIDIA only.


Rohan Abeyaratne. *Volume II of Lecture Notes on,The Mechanics of Elastic Solids: Continuum Mechanics*. http://web.mit.edu/abeyaratne/Volumes/RCA_Vol_II.pdf. [Online; accessed 08-November-2018]. MIT Department of Mechanical Engineering, 2012.


Klaus-Jürgen Bathe. *Finite element procedures*. Klaus-Jurgen Bathe, 2006.


Martha W Evans, Francis H Harlow, and Eleazer Bromberg. *The particle-in-cell method for hydrodynamic calculations*. Tech. rep. LOS ALAMOS NATIONAL LAB NM, 1957.


Ming Gao et al. "GPU Optimization of Material Point Methods". In: *ACM Trans. Graph.* 37.6 (2018), 254:1–254:12. ISSN: 0730-0301.


Johan Gaume et al. "Unified modeling of the release and flow of snow avalanches using the Material Point Method". In: Aug. 2018.


Chenfanfu Jiang et al. "The material point method for simulating continuum materials". In: *ACM SIGGRAPH 2016 Courses*. ACM. 2016, p. 24.


Fabian Meyer. "Simulation von Schnee". Bachelor's Thesis. Universität Koblenz-Landau, Institut für Computervisualistik, 2015.


NVIDIA Corporation. *NVIDIA Nsight*. https://docs.nvidia.com/nsight-visual-studio-edition/Content/Performance_Markers_OGL.htm. [Online; accessed 5-December-2018].


Michael Steffen, Robert M Kirby, and Martin Berzins. "Analysis and reduction of quadrature errors in the

material point method (MPM)". In: *International journal for numerical methods in engineering* 76.6 (2008), pp. 922–948.

Alexey Stomakhin et al. "A material point method for snow simulation". In: *ACM Transactions on Graphics (TOG)* 32.4 (2013), p. 102.

Deborah Sulsky, Shi-Jian Zhou, and Howard L Schreyer. "Application of a particle-in-cell method to solid mechanics". In: *Computer physics communications* 87.1-2 (1995), pp. 236–252.